Biochimica et Biophysica Acta, 1145 (1993) 93–104

BBAMEM 75845

Dehydration-induced lamellar-to-hexagonal-II phase transitions in DOPE/DOPC mixtures

Murray S. Webb [a], Sek Wen Hui [b] and Peter L. Steponkus [a]

[a] *Department of Soil, Crop and Atmospheric Sciences, Cornell University, Ithaca, NY (USA)* and [b] *Biophysics Department, Roswell Park Memorial Institute, Buffalo, NY (USA)*

(Received 13 April 1992)
(Revised manuscript received 17 September 1992)

Key words: Phosphatidylcholine; Phosphatidylethanolamine; Hexagonal II phase; Lyotropic phase behavior; Freezing stress; Dehydration

Plasma membranes of protoplasts isolated from non-acclimated rye plants undergo a transition from the bilayer to the inverted hexagonal (H_{II}) phase during freeze-induced dehydration at −10°C. It has been suggested (Bryant, G. and Wolfe, J. (1989) Eur. Biophys. J. 16, 369–372) that the differential hydration of various membrane components may induce fluid-fluid demixing of highly hydrated (e.g., PC) from poorly hydrated (PE) components during dehydration. This could yield a PE-enriched domain more prone to form the H_{II} phase. We have examined the lyotropic phase behavior of mixtures of DOPE and DOPC at 20°C by freeze-fracture electron microscopy, differential scanning calorimetry, and X-ray diffraction. H_{II} phase formation was favored by higher proportions of DOPE and lower water contents. Mixtures of 1:1 and 1:3 DOPE/DOPC had a hydration-dependent appearance of two L_α phases at water contents just above those at which the H_{II} phase occurred. The hydration-dependence of the lamellar repeat spacings suggested that the DOPE-enriched domains preferentially underwent the L_α-to-H_{II} phase transition. Mixtures of 3:1 DOPE/DOPC did not separate into two L_α phases during dehydration. These data suggest that the differential hydration characteristics of various membrane components may induce their lateral fluid-fluid demixing during dehydration.

Introduction

Severe dehydration during freezing is a major cause of injury in a wide variety of temperate climate plants [1,2]. Protoplasts that are isolated from leaves of non-acclimated rye plants (NA protoplasts) and frozen to −10°C undergo a reduction in volume of 85–90% as a result of water efflux because of the large gradient in the chemical potential of the extracellular ice and the supercooled cytosol. The vapor pressure of ice at this relatively 'high' sub-zero temperature is −12 MPa. Injury in these protoplasts is associated with the appearance of aparticulate lamellae subtending the plasma membrane, aparticulate domains in the plasma membrane, the close approach of a variety of cytoplasmic membranes, and ultimately of the hexagonal-II (H_{II}) phase in the plasma membrane and subtending lamellae [3] as well as in the chloroplast envelope and endomembranes [4]. These alterations in the ultrastructure of the plasma membrane can be effected in NA protoplasts by osmotic dehydration in a 5.3 osM sorbitol solution at 0°C [3]. Therefore, in NA protoplasts, the major stress during freezing at −10°C is due to dehydration rather than temperature reduction per se.

Amongst the commonly occurring phospholipid species in the rye plasma membrane, the unsaturated species of phosphatidylethanolamine (PE) have the greatest propensity to undergo the L_α-to-H_{II} phase transition. However, the content of unsaturated PE species in the plasma membrane of non-acclimated rye leaves is relatively low, at 11 mol% of the total lipid [5]. In this proportion, the PE is stabilized in the lamellar phase by the presence of the other lipids. However, lateral demixing of PE in the plane of the membrane could serve to locally enrich PE levels to proportions sufficient to facilitate H_{II} phase formation within iso-

Correspondence to: P.L. Steponkus, Department of Soil, Crop and Atmospheric Sciences, Cornell University, 608 Bradfield Hall, Ithaca, NY 14853, USA.

Abbreviations: DSC, differential scanning calorimetry; DOPC, dioleoylphosphatidylcholine; DOPE, dioleoylphosphatidylethanolamine; H_{II}, hexagonal-II; L_α, lamellar liquid crystalline; L_β, lamellar gel; T_{bh}, L_α-to-H_{II} phase transition temperature; T_m, L_α-to-L_β phase transition temperature.

lated domains. Crowe and Crowe [6] have proposed that the lateral enrichment of PE may be facilitated by a lyotropic L_α-to-L_β phase transition of phosphatidylcholine (PC) species. However, this phase separation appears not to occur in the rye plasma membrane at -10°C because the PC molecular species that predominate in the rye plasma membrane do not enter the L_β phase at those temperatures and hydrations encountered during freezing at -10°C [7]. Instead, it is possible that lateral enrichment of PE into a spatially separate domain occurs during bilayer dehydration because of differences in the hydration characteristics of the PE and PC headgroups [8]. Previously Rand [9] has proposed that fluid-fluid demixing might occur in mixed PC and PE systems during the close approach of vesicles or bilayers. The occurrence of fluid-fluid demixing during membrane dehydration might facilitate the L_α-to-H_{II} phase transition and would predict that the H_{II} phase would be enriched in PE and depleted in PC when the lamellar and H_{II} phases coexist.

Alternatively, the lyotropic L_α-to-H_{II} phase transition may proceed without either an L_α-to-L_β phase separation or fluid lipid-lipid demixing. Dehydration would decrease headgroup hydration to levels insufficient to maintain lipid headgroup packing and, hence, be unable to sustain the lamellar structure. At low hydrations the lipid monolayers would be expected to develop a spontaneous radius of curvature such that the free energy of the dehydrated bilayer would be minimized by sequestering the remaining water in the cores of the inverted cylindrical micelles of the H_{II} phase [10]. This phase change would have the structural effect of minimizing the surface area of the headgroups while maximizing the volume occupied by the acyl chains [10]. This mechanism would predict that lipid demixing would not necessarily precede the L_α–H_{II} transition and that all lipid components in the mixture would be proportionally represented in the H_{II} phase when the lamellar and H_{II} phases coexist. It should be noted that even lipids commonly considered to adopt only the lamellar phase, such as egg PC, can undergo lamellar-to-H_{II} phase transitions at very low hydrations and elevated temperatures [11]. In general, the distinction between those lipids that are considered as bilayer-forming from those that are non-bilayer forming has been made from consideration of their thermotropic phase behavior in excess water and may not be appropriate for lyotropic events.

This study was undertaken to determine what structural changes occur in DOPE/DOPC bilayers as a result of dehydration that might facilitate the lyotropic L_α-to-H_{II} phase transition. Specifically, in mixtures containing sufficient DOPC to stabilize the L_α phase of fully hydrated bilayers containing DOPE, it was of interest to determine if DOPE and DOPC remained well mixed during dehydration. However, if DOPE and DOPC demixed during dehydration, we wished to determine if this demixing occurred as either a result of (1) a lyotropic L_α-to-L_β phase transition of DOPC or (2) fluid phase immiscibility as a consequence of the hydration differences between DOPE and DOPC. Therefore, we have examined the phases adopted by DOPE/DOPC mixtures dehydrated at vapor pressures that are equivalent to the vapor pressure of ice at temperatures over the range of -2°C to -40°C.

Materials and Methods

Desorption isotherms and differential scanning calorimetry

Lipids, which were obtained from Avanti Polar Lipids (Birmingham, AL), were used without additional purification. Pure lipids or lipid mixtures were first mixed in $CHCl_3$ and then the solvent was removed under a stream of N_2 gas at 40°C. Residual solvent was removed under high vacuum for at least 2 h and usually overnight. Samples prepared for desorption and differential scanning calorimetry (DSC) were dispersed at 12–15 wt% lipid in double-distilled H_2O that was first degassed under vacuum and then saturated with N_2. Samples were dispersed by a combination of vortexing and mild sonication as well as thermal cycling between 4°C and 55°C. Lipids were maintained under N_2 for the entire dispersal procedure. After the initial hydration, the lipids were allowed to equilibrate for a further 6–8 h at 4°C. At the end of this period, aliquots of the multilamellar dispersions were placed into preweighed DSC pans and desorbed above various saturated salt solutions in a N_2 atmosphere for seven days at 20°C. At the end of this equilibration period the pans were sealed and re-weighed. DSC was performed on all hydrated and dehydrated dispersions using a Perkin-Elmer DSC-7 using a temperature program of cooling from 20 to -40°C at 10 C°/min (except where indicated) followed by immediate warming to 20°C at the same rate. In all cases, reported values for the peak of the L_β-to-L_α phase transition temperature (T_m) and transition enthalpy were calculated using the DSC-7 software. After the DSC experiments, lipid dry weights were obtained by opening the DSC pans and allowing complete desiccation to occur by sample incubation for 16 h over P_2O_5 in a vacuum oven maintained at 70°C. All water contents are expressed as wt% water as follows:

$$\text{wt\% water} = \left[\frac{\text{g water}}{\text{g water} + \text{g lipid}}\right] \cdot 100$$

assuming that no water remained in the dispersions dehydrated over P_2O_5. Samples were periodically checked for the occurrence of acyl chain oxidation during the desorption period by re-extraction of the

dried lipids into $CHCl_3$ followed by thin-layer chromatography and H_2SO_4 charring. Results obtained from samples showing any detectable lipid oxidation products were not used.

Salts used for the desorption were: Na_2HPO_4, KNO_3, $BaCl_2$, KCl, NaCl, NaBr, $Mg(NO_3)_2$, $MgCl_2$, and LiCl. At 20°C, the vapor pressures for these salts are: −2.7, −8.3, −12.8, −20.4, −38.9, −76.1, −88.5, −150, and −286 MPa, respectively. These values were calculated from published relative humidity data [12] using the equation:

$$\psi = \frac{RT}{V_w} \cdot \ln\left[\frac{RH}{100}\right]$$

where ψ = the vapor pressure in MPa; V_w is the partial molar volume of water ($18 \cdot 10^{-6}$ m^3); RH is the relative humidity, R is the gas constant (8.3143 J/mol per K) and T is the temperature (293 K).

Freeze-fracture electron microscopy

Samples for freeze-fracture electron microscopy were prepared and desorbed as described above except that the lipids were initially dispersed at approx. 50 wt% in water. Aliquots of 3–5 μl of these lipids were placed directly on the freeze-fracture sample holders and desorbed at 20°C. At the end of the equilibration period, samples were quenched in liquid propane supercooled with liquid nitrogen. Total time of exposure of the desorbed samples to the ambient atmosphere was 4–6 s. We have ensured that the wt% water values obtained by desorbing lipids on freeze-fracture sample holders were identical to those obtained from lipids desorbed in DSC pans as follows. Lipid samples were dispersed at 50 wt% and desorbed on pre-weighed freeze-fracture sample holders placed inside pre-weighed DSC pans. After the equilibration time, the wet and dry weights of the samples were obtained as described above and the weight of the DSC pans and freeze-fracture holders subtracted to determine the water content of lipids dehydrated on freeze-fracture stubs.

Samples were fractured and replicated in a Balzers 400K instrument at $< 2 \cdot 10^{-7}$ torr and −107°C. Replicas were washed in $CHCl_3/CH_3OH$ (1:2, v/v) for 2–3 h then transferred directly onto uncoated grids and examined in a Philips EM300 electron microscope at 80 kV accelerating voltage.

Calculation of d spacings for the H_{II} phase

Center-to-center repeat spacings (d spacing) of the H_{II} lattice were determined by measurements of the H_{II} cylinders from electron micrographs enlarged to $\geqq 100\,000\times$. Data were obtained with a micrometer using a 'blind' method in which neither the dispersion identity and water content nor the print magnification were known before the measurements were made. Spacings were calculated by measurement of the width, in nm, of 10–20 inverted cylindrical micelles then dividing by the number of H_{II} cylinders to obtain an average center-to-center cylinder repeat spacing. Such a determination constituted a single measurement. Reported values represent the averages (± standard deviation) of at least ten (usually $\geqq 30$) such measurements obtained in this manner totaling at least 100 (usually 200–600) H_{II} cylinders.

X-ray diffraction

DOPE/DOPC mixtures, which were dispersed in excess water (85 wt% water) as described, were loaded into pre-weighed X-ray capillary tubes by using a Bio-Rad Gel Tube Extrusion needle. Dispersions were first dehydrated under vacuum to the desired water contents and then the tubes were flushed with N_2 gas, sealed, and allowed to equilibrate in the vapor phase for 5–7 days at 22°C. Samples were examined at 21° to 22°C by both wide-angle and small angle X-ray diffraction using a Rigaku 300H rotating anode X-ray generator with a copper target and a Frank-type camera. The diffractions were recorded on Kodak DEF-5 X-ray film or by a TEC position-sensitive wire detector and a PCA analyzer. The camera length was calibrated using a nanodecane standard at 10°C.

Results

Hydration characteristics

After desorption of aqueous dispersions of DOPE, DOPC, and the 3:1, 1:1, and 1:3 (mol/mol) mixtures of these lipids above saturated salt solutions, the water content of the lipids decreased linearly with the ln of the vapor pressure (Fig. 1). The linear relationship of

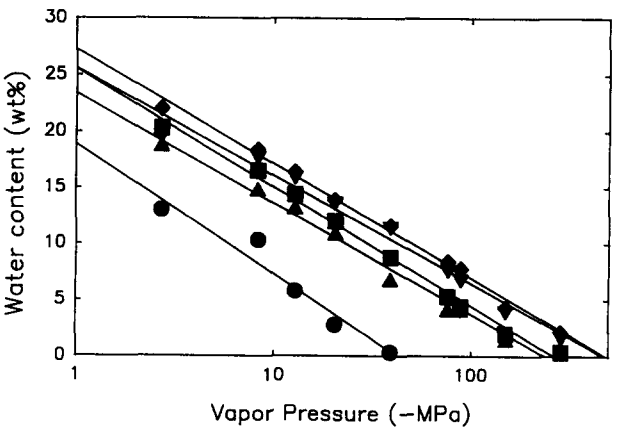

Fig. 1. Desorption isotherms for DOPE (●), DOPC (♦), and DOPE/DOPC mixtures in the molar proportions of 3:1 (▲), 1:1 (■), and 1:3 (▼). Desorption was performed at 20°C over saturated salt solutions under an N_2 atmosphere. Water contents were determined gravimetrically.

water content with the ln of the vapor pressure indicates that the water content of bilayers follows the exponential decay of repulsive hydration forces with distance between bilayer surfaces [13]. Data in Fig. 1 show that pure DOPC is significantly more hydrated than pure DOPE at equivalent vapor pressures. At a vapor pressure of −13 MPa, the water content of DOPC was 16.8 wt% and 6.7 wt% for DOPE. Values for the water content of DOPE were similar to those reported previously for DOPE dispersions that were osmotically dehydrated [14]. The vapor pressures required for the lipid to reach zero wt% water, P_0, were significantly different between DOPC (−380 MPa) and DOPE (−73 MPa). Other workers have reported very similar P_0 values of −398 MPa measured for DOPC at 25°C [15] and −73 MPa for DOPE, which was calculated from the data of Rand et al. (Ref. 14, Table VIII). This difference in hydration between PE and PC is that predicted to facilitate lipid-lipid demixing during dehydration [8,9].

The water content of the desorbed lipid dispersions increased non-linearly with the addition of DOPC to DOPE (Fig. 2). For example, after equilibration at −13 MPa, the water contents of the dispersions were 6.7, 13.2, 14.4, 15.9, and 16.8 wt% for 0, 25, 50, 75, and 100 mol% DOPC in DOPE, respectively. This non-linear relationship between water content and DOPC content was found at all vapor pressures examined (Fig. 2). The non-linear increase in hydration with addition of DOPC to DOPE could result from either a higher hydration of the L_α phase (stabilized by the presence of 25 mol% DOPC (Fig. 11)) than the H_{II} phase or from a higher affinity of DOPC for water than that for DOPE (Figs. 1 and 2). However, this difference in water content cannot be entirely attributed to a greater hydration for the lamellar phase than for the H_{II} phase because the hydration of DOPE in the L_α phase (2°C) is significantly lower than that of DOPC or N-methylated DOPE analogues in the same phase [16]. Rather, the lower water contents of DOPE dispersions relative to those containing DOPC demonstrate the lower water affinity of the DOPE head group [17]. In addition, these data indicate that in DOPE/DOPC mixtures, the H_{II} phase is not more hydrated than the L_α phase under conditions in which the L_α-to-H_{II} phase transition is elicited by dehydration. That is, no discontinuities in the desorption isotherms (Fig. 1) were observed at the water contents at which the L_α-to-H_{II} phase transitions occurred (Figs. 3–5, 11). A higher hydration of the H_{II} phase relative to the L_α phase has been reported for some PE systems [18]. In this respect, lyotropic transitions are distinct from those occurring thermotropically in excess water.

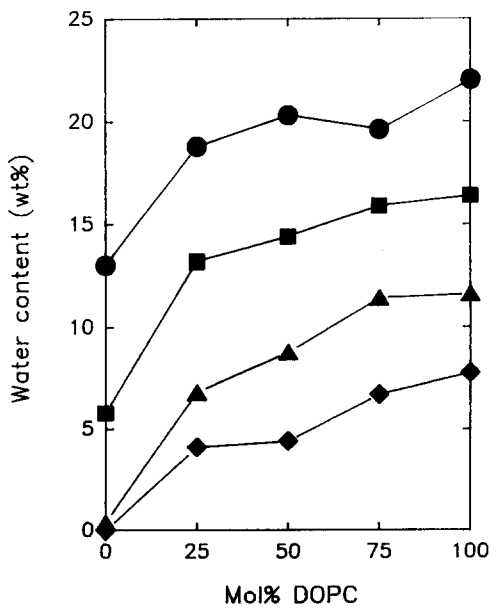

Fig. 2. Plot of the water content of DOPE, DOPC, and their 3:1, 1:1, and 1:3 mixtures as a function of vapor pressure. Curves represent water contents after desorption at −2.7 MPa (●), −12.8 MPa (■), −38.9 MPa (▲) and −88.5 MPa (◆).

Freeze-fracture electron microscopy

The effect of dehydration on the occurrence of the H_{II} phase in these lipid dispersions has been performed by freeze-fracture electron microscopy. The L_α-to-H_{II} phase transition temperature (T_{bh}) of pure DOPE is between 5°C and 10°C at full hydration [19]. Because the T_{bh} value is decreased at lowered water contents [18], DOPE is expected to be in the H_{II} phase under all conditions examined here; therefore freeze-fracture experiments on desorbed DOPE were not conducted. In a 3:1 DOPE/DOPC mixture, the lamellar phase existed at water contents $\geq$ 12.5 wt% water (not shown). After equilibration at a vapor pressure of −39 MPa, the 3:1 DOPE/DOPC dispersions contained 7.7 wt% water and both lamellar (Fig. 3a) and H_{II} (Fig. 3b) phases were present. At water contents $\leq$ 4.2 wt% only the H_{II} phase existed. In 1:1 DOPE/DOPC dispersions, only the lamellar phase existed at water contents > 8.8 wt%. Both lamellar (Fig. 4a) and H_{II} (Fig. 4b) phases were observed in samples containing between 5.7 wt% water (−76 MPa) and 5.0 wt% water (−88 MPa); at water contents $\leq$ 2.6 wt%, only the H_{II} phase was observed. In the 1:3 DOPE/DOPC dispersions more extensive dehydration was required for the formation of the H_{II} phase. This mixture was in the lamellar phase at all water contents $\geq$ 6.9 wt% water (−88 MPa). At 4.7 wt% water (−150 MPa) both lamellar and H_{II} phases were observed (Fig. 5), and only the H_{II} phase was observed at hydrations $\leq$ 2.1 wt% water. Although DOPC forms the H_{II} phase at very low water contents

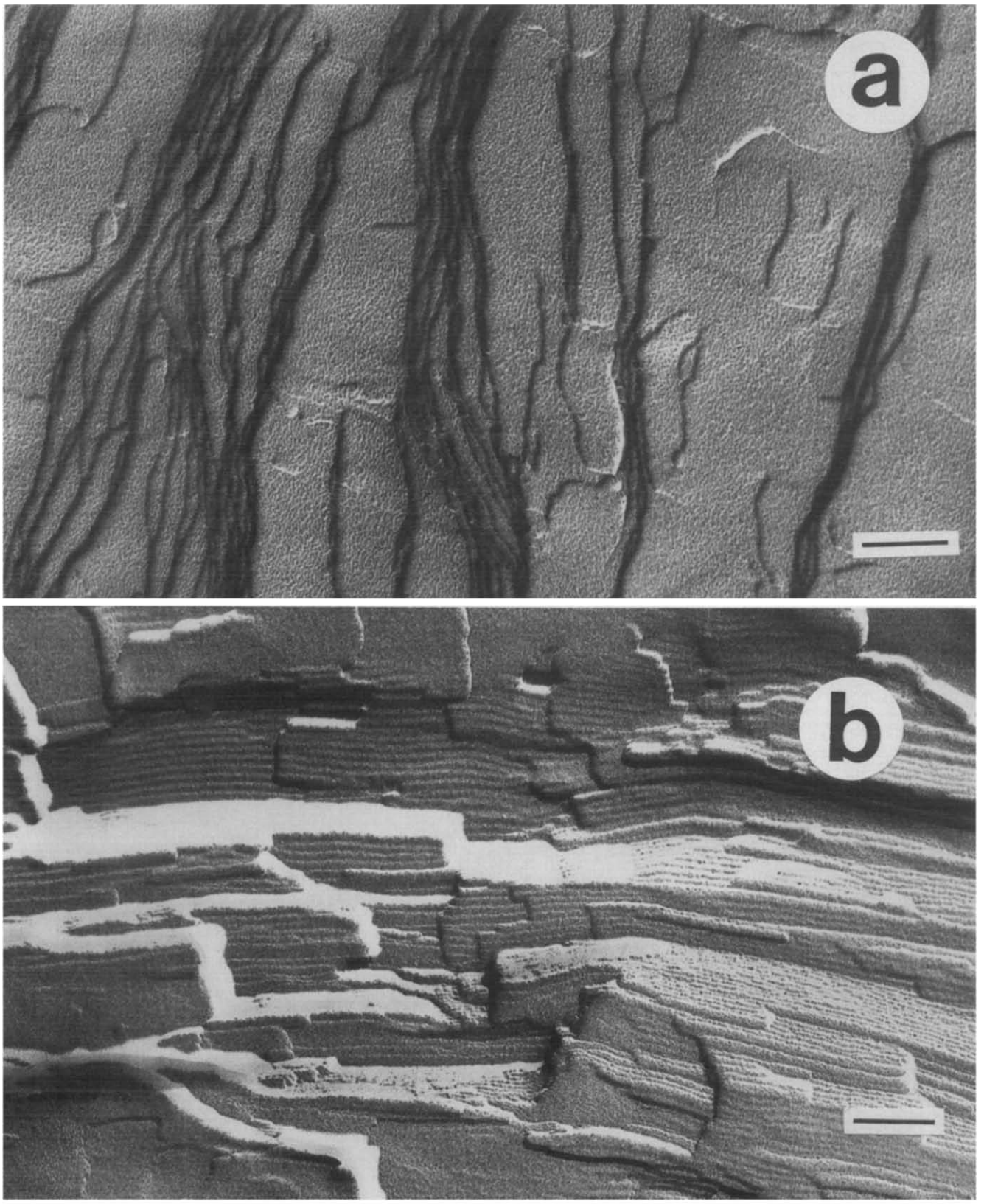

Fig. 3. Representative freeze-fracture electron micrographs of DOPE/DOPC (3:1) desorbed at −39 MPa and 20°C. The dispersion had co-existing L_α (3a) and H_{II} (3b) phases. Bars represent 100 nm.

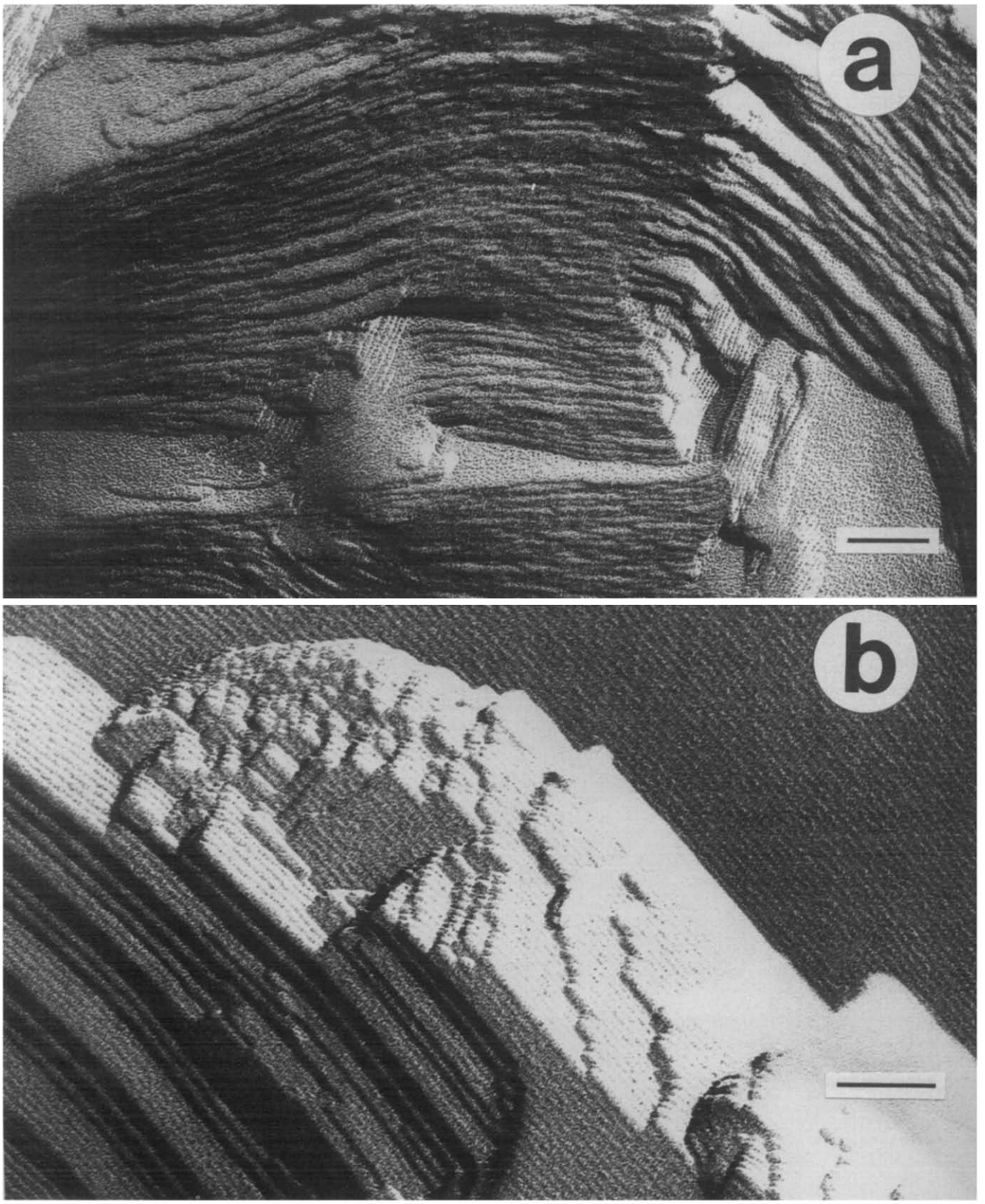

Fig. 4. Representative freeze-fracture electron micrographs of DOPE/DOPC (1:1) desorbed at −88 MPa and 20°C. The dispersion had co-existing L_α (4a) and H_{II} (4b) phases. Bars represent 100 nm.

[11], we observed only the lamellar phase in our samples at water contents $\geqq 3.0$ wt% at 20°C.

Differential scanning calorimetry

Differential scanning calorimetry was performed on DOPE, DOPC, and their binary mixtures dispersed in excess water. The L_β-to-L_α phase transition temperatures, which were determined during heating of the lipids in excess water, were −8.1°C, −10.1°C, −13.1°C, −15.5°C, and −17.7°C for DOPE, 3:1, 1:1, 1:3 (DOPE/DOPC), and DOPC, respectively. Calculated transition enthalpies were 31.7, 34.8, 33.8, 33.7 and 34.2 kJ/mol, respectively. These T_m and enthalpy values for DOPC are very similar to those summarized by Marsh [20] for DOPC in excess water, and the T_m for DOPE is similar to that reported by Gruner et al. [16].

To determine if the lamellar phase observed by freeze-fracture electron microscopy represented either the L_α or L_β phase, DSC thermograms were obtained for lipid dispersions dehydrated to water contents between 4.5 wt% and 22 wt%. For all mixtures, a single lipid transition was observed in the heating scans. Further, at all water contents $\geqq 5$ wt%, the large enthalpies of the observed endotherms indicated that the transition was the L_β-to-L_α phase transition rather than the low-enthalpy L_α-to-H_{II} phase transition. A plot of transition temperature vs. water content for the desorbed dispersions shows that the transition temperature increased with decreasing hydration for both the pure lipids and the lipid mixtures (Figs. 6a–e). This behavior has been reported previously for the T_m of the L_β-to-L_α transition in PC systems [21]. For all of these mixtures the DSC data indicated that the temperature of the main gel-liquid crystalline phase transition was $\leqq 0$°C (Figs. 6a–e). This indicates that all lamellar phases observed by freeze fracture electron microscopy in samples desorbed at 20°C (Figs. 3–5) were in the liquid crystalline lamellar (L_α) phase. This conclusion was confirmed by wide-angle X-ray diffraction of DOPE/DOPC dispersions dehydrated to water contents between 50 wt% and 1.2 wt%.

Plots of the enthalpies of the phase transitions determined from the DSC heating endotherms vs. the water content of the dispersion are also shown in Figs. 6a–e. These results showed that the transition enthalpies for these dispersions were 30–35 kJ/mol at all water contents $\geqq 12$ wt% (Figs. 6a–e). In DOPC, the transition enthalpy decreased linearly from 32 to 21 kJ/mol with decreasing hydration between 17 wt% and 4.5 wt% water (Fig. 6e). For DOPE and all of the DOPE/DOPC mixtures, the transition enthalpies decreased to approx. 25 kJ/mol at hydrations between 12 wt% and 5 wt% water, regardless of the DOPE content (Figs. 6a–d). Because a decrease in enthalpy to 25

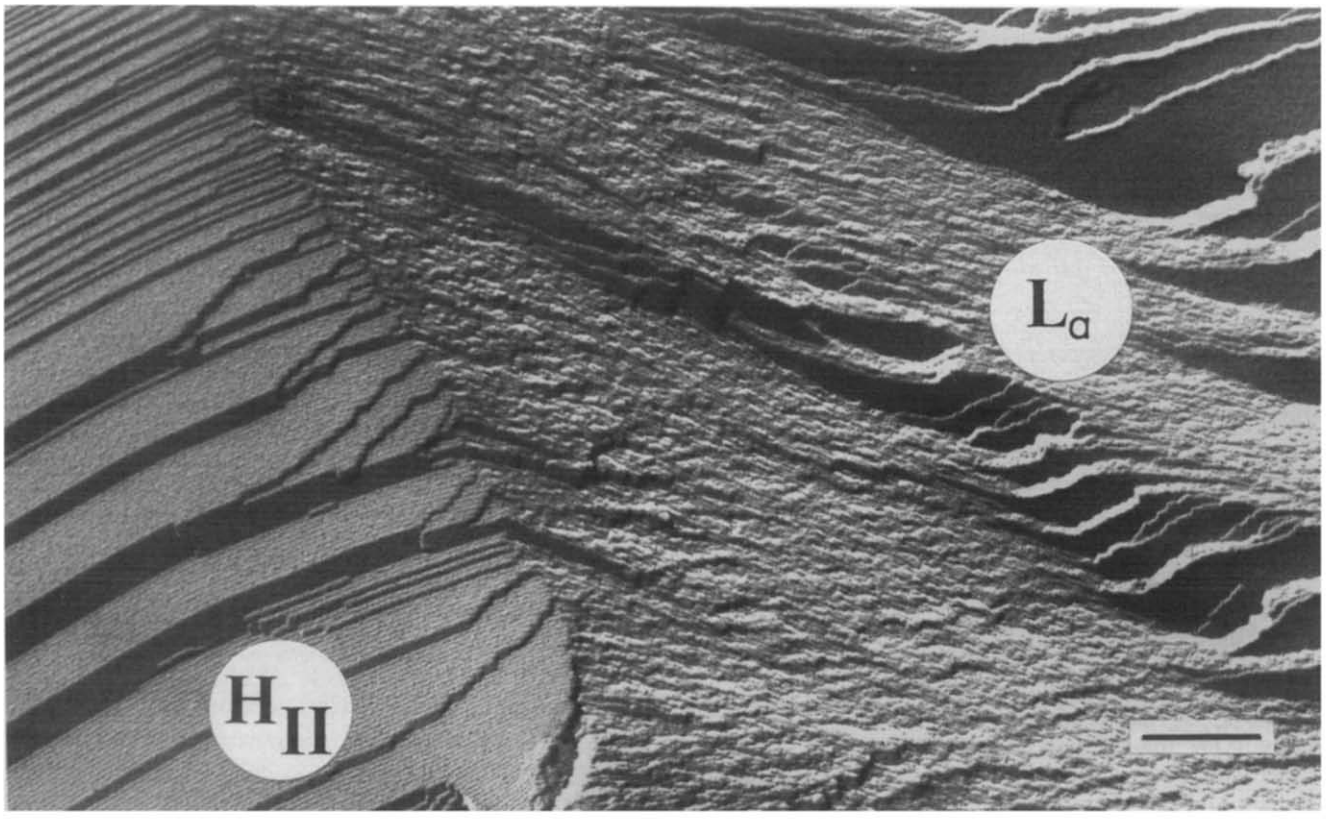

Fig. 5. Representative freeze-fracture electron micrograph of DOPE/DOPC (1:3) desorbed at −150 MPa and 20°C. The dispersion had co-existing L_α and H_{II} phases. Bar represents 200 nm.

kJ/mol was observed in both DOPE and DOPC, which were in the H_{II} and L_α phases, respectively, at all water contents, as well as in the lipid mixtures, the decrease in enthalpy probably represents a dehydration-dependent decrease in the L_β-to-L_α transition enthalpy and was not a consequence of the trapping of lipid in the H_{II} phase during the DSC cooling cycle. However, to ensure that the thermodynamic parameters presented in Fig. 6 were not consequences of non-equilibrium phase transitions due to the relatively high scan rate of 10 C°/min, we have repeated the

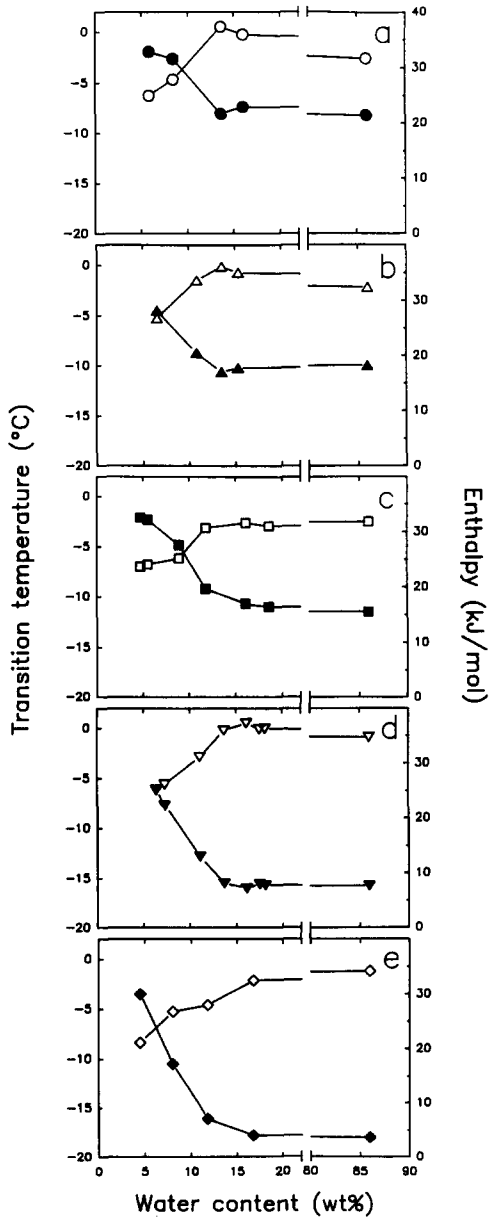

Fig. 6. Temperature (filled symbols) and enthalpy (open symbols) of the observed phase transitions vs. water content (wt%) for desorbed DOPE (a); DOPE/DOPC, 3:1 (b); DOPE/DOPC, 1:1 (c); DOPE/DOPC, 1:3 (d); and DOPC (e). Transition enthalpy per mole of total lipid was determined from the main endotherm observed during warming scans.

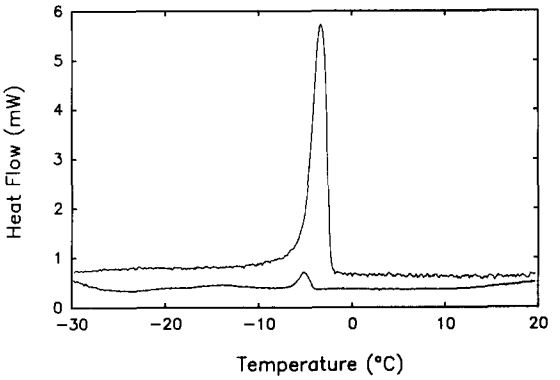

Fig. 7. DSC scans of DOPE/DOPC (1:1) equilibrated at −76.1 MPa. The upper curve represents a dehydrated lipid mixture scanned at 10 C°/min. This sample had a water content of 5.72 wt%, a T_m of −3.6°C and a transition enthalpy of 25.2 kJ/mol. The lower curve represents a dehydrated lipid mixture scanned at 0.5 C°/min. This sample had a water content of 5.82 wt%, a T_m of −5.2°C and a transition enthalpy of 23.4 kJ/mol. Both traces represent the original DSC scans and are neither computer-smoothed nor have had background noise subtracted. A comparison of the T_m and enthalpy reported here at 10 C°/min with those shown in Fig. 6c for other 1:1 DOPE/DOPC samples at similar water contents indicates the high reproducibility of these thermodynamic parameters.

DSC studies with samples at very slow scan rates (Fig. 7). At water contents greater than 4.5 wt%, the transition temperatures determined at 10 C°/min were very similar to those determined at 0.5 C°/min (Fig. 7). The more rapid scan rate reported a transition temperature only 1.5 C° higher than that determined at 0.5 C°/min. Similarly, the calculated transition enthalpies were not significantly affected by the scan rate (Fig. 7). At water contents lower than 4.5 wt%, the 10 C°/min scan rate underestimated the transition enthalpy (data not plotted). Presumably this occurred as a result of the dehydrated lipids not undergoing an equilibrium phase transition at this scan rate. Alternatively, the presence of only the H_{II} phase at water contents below ≈ 4.5 wt% (Fig. 11) may cause the $H_{II} \rightarrow L_\alpha$ to be slow or absent at these hydrations and 10 C°/min scan rates. In either case, above 4.5 wt% water the thermodynamic parameters obtained at 10 C°/min are accurate estimates of the equilibrium phase transition values and we report only those values. Nevertheless, these data clearly demonstrate that the $L_\beta \rightarrow L_\alpha$ phase transition occurred at temperatures at least 20 C° lower than the temperature at which the lipids were dehydrated and analyzed in the freeze-fracture and X-ray diffraction studies (Fig. 3–5, 8–10). Therefore, the lamellar phases observed in samples at 20°C by freeze-fracture electron microscopy represent the L_α phase.

X-ray diffraction

To test for the occurrence of dehydration-dependent fluid lamellar phase demixing, mixtures of DOPE/DOPC were dehydrated to water contents be-

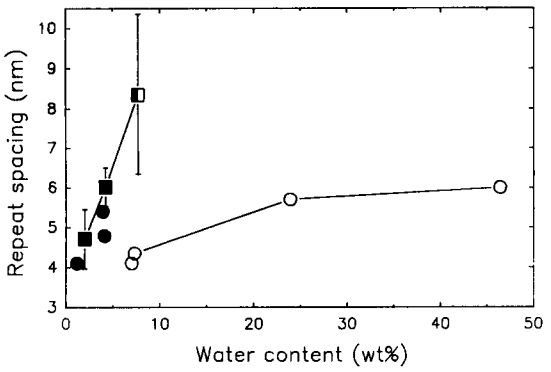

Fig. 8. Lamellar and center-to-center H_{II} repeat spacings for dehydrated dispersions of DOPE/DOPC 3:1. Spacings and phases were determined by freeze-fracture electron microscopy (squares) and X-ray diffraction (circles). Water contents for freeze-fracture samples were obtained by interpolation of the data presented in Fig. 1. Closed symbols represent samples with only the H_{II} phase; open symbols indicate samples with only the L_α phase(s); and half-closed symbols denote the presence of both the L_α and H_{II} phases.

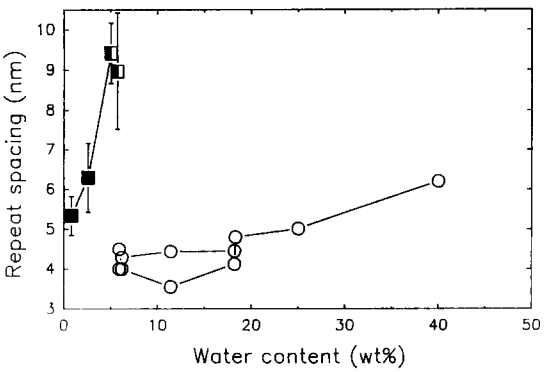

Fig. 9. Lamellar and center-to-center H_{II} repeat spacings for dehydrated dispersions of DOPE/DOPC 1:1. Symbols as described in the legend to Fig. 8.

tween 50 wt% and 1.2 wt% at 22°C and examined by X-ray diffraction. At all hydration levels, a diffuse wide-angle Bragg reflection centered at a spacing of 0.46 nm, which is characteristic of disordered acyl chains in the L_α phase, was observed and the sharp Bragg reflection at 0.42 nm, characteristic of ordered acyl chains in the L_β phase, did not occur. This result is consistent with the DSC data described above and indicates that all samples were in the fluid phase at all water contents; no fluid-gel phase separation occurred as a result of dehydration.

In the small-angle region, diffractions were measured for their repeat spacings and indexed to either the lamellar, hexagonal, or cubic phases. In the 3:1 DOPE/DOPC mixture, the L_α phase was present at water contents of 46, 24, 7.3 and 7.0 wt%. Over this range of water contents, the lamellar repeat spacing decreased from 6.0 nm to 4.1 nm (Fig. 8). At water contents $\leqq$ 4.5 wt% only the H_{II} phase was present as detected by both freeze-fracture electron microscopy and by X-ray diffraction. In the 3:1 DOPE/DOPC mixture, the mean H_{II} repeat spacing at 7.7 wt% water was 8.3 nm, a value similar to the largest d spacing of 7.5 nm obtained for a fully hydrated mixture of DOPE/DOPC (3.17:1) in the H_{II} phase at 50–55°C, as measured by X-ray diffraction [19]. There was no evidence for the occurrence of fluid-fluid lamellar phase demixing in the 3:1 DOPE/DOPC dispersions as a function of dehydration.

At 40 wt% water, the 1:1 DOPE/DOPC mixture was in the L_α phase with a repeat spacing of 6.20 nm; at 25 wt% water it was also in the L_α phase with a repeat spacing of 5.01 nm (Fig. 9). Between 18 wt% and 6.4 wt% the diffractions resolved into two separate L_α spacings. The difference between these spacings was maximal at 11 wt% water (4.44 nm and 3.55 nm) and reached a minimum at 6 wt% water (4.29 nm and 4.00 nm), a water content just above that at which the H_{II} phase was first observed (Fig. 9). A similar separation of a single L_α phase into two separate L_α phases was observed during the dehydration of 1:3 DOPE/DOPC dispersions. In the 1:3 DOPE/DOPC mixtures, L_α phases were detected between 49 wt% (repeat spacing of 6.30 nm) and 24 wt% water (5.10 nm) (Fig. 10). At a hydration of 4.5 wt% water, freeze-fracture electron microscopy data indicated the simultaneous co-existence of both L_α and H_{II} phases and exclusively the H_{II} phase at 1.2 wt% water (Fig. 10). At several water contents just higher than that at which the H_{II} phase was first observed (5.5–7.0 wt%), X-ray diffraction data indicated the presence of two separate L_α phases with typical spacings of 4.40 and 5.20 nm (Fig. 10).

A diagram of the phase structures adopted by DOPE, DOPC and their mixtures desorbed at 20°C is given in Fig. 11. The diagram was constructed from phase determinations made by freeze-fracture electron microscopy, DSC and X-ray diffraction. The occurrence of the H_{II} phase was dependent on both water content and the proportion of DOPE in the mixture.

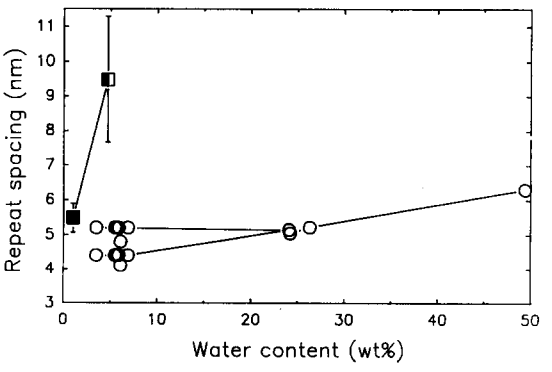

Fig. 10. Lamellar and center-to-center H_{II} repeat spacings for dehydrated dispersions of DOPE/DOPC 1:3. Symbols as described in the legend to Fig. 8.

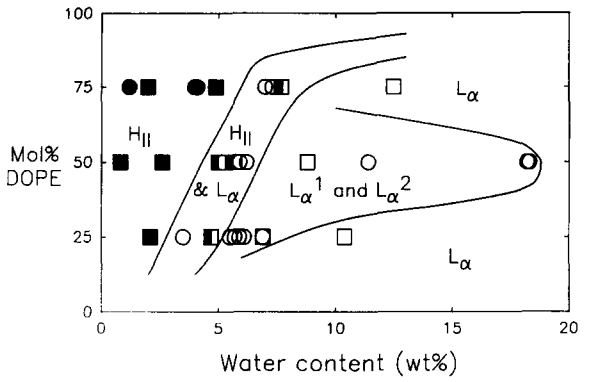

Fig. 11. Diagram of the phase structure of DOPE/DOPC mixtures as a function of water content at 20°C. Symbols are as described in the legend to Fig. 8; L_α^1 and L_α^2 denote demixed fluid lamellar phases.

The H_{II} phase was promoted by higher DOPE levels and/or lower water contents. Over the range of 0–75 mol% DOPE, the water content at which the H_{II} phase was first observed increased with increasing mol% DOPE in the mixture. It can be seen that there are a wide variety of combinations of DOPE and water contents at which both the L_α and H_{II} phases can co-exist (Fig. 11). It should be noted, however, that the positions of these phase boundaries are not known precisely. Finally, Fig. 11 summarizes the occurrence of two separate L_α phases (designated L_α^1 and L_α^2 in Fig. 11) in dehydrated 1:1 and 1:3 DOPE/DOPC dispersions.

Discussion

The purpose of this study was to determine what phase and miscibility changes take place in DOPE/DOPC bilayers during isothermal dehydration. It was of interest to ascertain if DOPE and DOPC species either demixed or remained well mixed during bilayer dehydration preceding the lyotropic L_α-to-H_{II} phase transition. Further, if DOPE-DOPC demixing occurred during dehydration, we wished to determine if it was the result of fluid-fluid or fluid-gel phase separation. Previously, Crowe and Crowe proposed that a lyotropic L_α-to-L_β phase separation of PC may facilitate the local enrichment of PE species to levels sufficient for H_{II} phase formation [6]. This mechanism was proposed to explain the occurrence of the H_{II} phase in dehydrated bilayers containing relatively low proportions of PE. Alternatively, a theoretical analysis has suggested that lipids of markedly different hydration characteristics might undergo fluid-fluid phase separation (i.e., demixing) as a result of dehydration [8]. Bryant [22] has reported the occurrence of two lamellar repeat spacings at 308 to 310 K in 1:1 mixtures of 1-palmitoyl-2-oleoyl-PE and 1-palmitoyl-2-oleoyl-PC containing 10 wt% ^2H_2O. Although this temperature was only slightly above the peak of the L_α-to-L_β phase transition (305 K) for this mixture at 10 wt% ^2H_2O, X-ray diffraction data suggested that the L_β-phase was absent in these samples. The presence of the two lamellar repeat spacings was interpreted as demonstrating the occurrence of fluid-fluid demixing between PC and PE induced by dehydration [22].

In this report, we have examined dehydrated mixtures of unsaturated species of PE and PC at temperatures well above the L_α-to-L_β phase transition temperature. The presence of two separate L_α repeat spacings occurring as a function of decreasing water content in both 1:1 and 1:3 mixtures of DOPE/DOPC indicates that these dispersions undergo fluid-fluid demixing during dehydration (Figs. 9 and 10). The lamellar repeats did not arise from a lyotropic L_α-to-L_β phase separation as both DSC (Fig. 6) and wide-angle X-ray diffraction data (not shown) indicated the absence of the L_β phase in these dispersions at any hydration at 20°C. A similar hydration-dependent appearance of two lamellar phases has been reported in DOPE/DOPC 1:1 mixtures in which the lipid was hydrated instead of dehydrated [23]. Our results differ from those of Tamura-Lis et al. [23] only in that they observed two separate lamellar spacings between 20 and 30 wt% water, whereas we observed such separations between 6 and 18 wt% water. In the work reported here, the DOPE/DOPC dispersions were dehydrated from excess water in which the lipids were initially well mixed. Therefore, the separation of a single L_α phase into two L_α phases occurred solely as a consequence of dehydration. Further, the hydration-dependent occurrence of two separate lamellar repeat spacings is not observed in either DOPC or egg PE at 25°C over the same water content range [15].

In contrast to the 1:1 and 1:3 DOPE/DOPC mixtures, there was no evidence for fluid-fluid demixing during dehydration of the 3:1 DOPE/DOPC mixture (Fig. 8). Similarly, Rand et al. have reported a single L_α phase in 3:1 DOPE/DOPC dispersions at hydrations $\geq$ 17 wt% [14]. These results indicate that, in dehydrated bilayers, small proportions of DOPC (25 mol%) are more miscible in DOPE than are small proportions of DOPE (25 mol%) in DOPC.

It is likely that the smaller lamellar spacings in dehydrated 1:1 and 1:3 DOPE/DOPC dispersions represent a DOPE-enriched bilayer and that the larger spacing represents a DOPC-enriched bilayer. This is consistent with the observation that the equilibrium interbilayer separations between PE bilayers are significantly smaller than those between PC bilayers [24]. In the dehydrated 1:1 mixture of DOPE/DOPC, an increase in the repeat spacing of the putatively DOPE-enriched domain occurred as a result of dehydration from 11 wt% water to 6 wt% water, which is just above

the water content at which the H_{II} was first observed (Fig. 9). This suggests that the DOPE-enriched domain was more prone to undergo the transition to the H_{II} phase because a preferential partitioning of DOPE from the DOPE-enriched lamellar domain to the H_{II} phase would result in higher proportions of DOPC remaining in this lamellar domain and, hence, in an increased lamellar spacing (Fig. 9). A similar increase in the lamellar phase repeat spacing and decrease in the H_{II} phase repeat spacing at the L_α-to-H_{II} phase transition has been observed in a 3.17:1 DOPE/DOPC dispersion in excess water [19].

The phase assignments for various DOPE/DOPC mixtures as a function of water content (Fig. 11) are consistent with data reported previously for other DOPE/DOPC mixtures. Bryant [22], using ^{2}H-NMR of DOPE/DOPC dispersions in 4.9 wt% ^2H_2O at 22°C, found co-existing L_α and H_{II} phases in 6:4 and 2:1 DOPE/DOPC dispersions, but only the L_α phase in 1:2 and 27:73 DOPE/DOPC dispersions. A 2:1 DOPE/DOPC dispersion containing 9 wt% ^2H_2O at 22°C was predominantly in the L_α phase, but also contained a small proportion of H_{II} phase [22]. Eriksson et al. [25] examined DOPE/DOPC dispersions in 10 wt% ^2H_2O by ^{31}P-NMR and ^{2}H-NMR. At 25°C, dispersions containing $\leqq 50$ mol% DOPE were exclusively in the L_α phase, whereas those with 67 and 75 mol% DOPE had co-existing L_α and H_{II} phases. Finally, Bradshaw et al. [26], using X-ray diffraction, found the L_α phase occurred in 3:7 DOPE/DOPC at 30°C at relative humidities $\geqq 75\%$ (-39 MPa $\approx$ 10 wt% water). In addition, these workers observed the occurrence of the H_{II} phase in the 3:7 DOPE/DOPC dispersion (30°C) at approx. 38% relative humidity ($\approx$ 5 wt% water). At 20°C and 5 wt% water, the 1:3 DOPE/DOPC dispersion contained both L_α and H_{II} phases (Fig. 11). The difference in phase adopted for the 1:3 dispersion at 20°C (Fig. 11) and that of Bradshaw et al. [26] for the 3:7 dispersion at 30°C is likely due to the promotion of the H_{II} phase by the higher temperature in the latter study.

The hydration at which the onset of the co-existence of the L_α and H_{II} phases occurred was lower for the 1:3 DOPE/DOPC dispersion than for the 3:1 DOPE/DOPC dispersion. Although the center-to-center distance of the inverted cylindrical micelles of the 1:3 dispersion was larger at the onset of the co-existence of the lamellar and H_{II} phases, the radius (R_w) of the water-filled cylinder, as calculated from the center-to-center distance and the fraction volume of water [27], was smaller. The values for R_w at the onset of co-existing L_α and H_{II} phases were 1.21, 1.10, and 1.08 nm for the 3:1, 1:1 and 1:3 dispersions of DOPE/DOPC, respectively. The small radius of the water cylinders in co-existing H_{II} and bilayer structures implies a high bending energy in the bilayer at equilibrium. The bending energy per molecule of the bilayers in equilibrium with H_{II} were estimated to be $2.7 \cdot 10^{-21}$, $3.2 \cdot 10^{-21}$ and $3.4 \cdot 10^{-21}$ Joules, respectively, for these bilayers [28]. This analysis shows that monolayer leaflets having higher PC contents may tolerate a higher bending energy before formation of the H_{II} phase. Therefore, PC stabilizes bilayers.

In summary, we have examined the phase behavior of mixtures of DOPE and DOPC at vapor pressures similar to those encountered by rye protoplasts during freezing to temperatures over the range of -2°C to -40°C. The L_α-to-H_{II} phase transition in DOPE/DOPC mixtures is both hydration- and lipid-composition dependent. We have demonstrated that the lyotropic L_α-to-H_{II} phase transition in DOPE/DOPC mixtures was not preceded by an L_α-to-L_β-induced phase separation of DOPC. Rather, the X-ray diffraction studies demonstrated that the lyotropic L_α-to-H_{II} phase transition in 1:1 and 1:3 mixtures of DOPE/DOPC is preceded by fluid-fluid phase demixing. This fluid-fluid lipid demixing results from the different hydration characteristics of PC and PE [8]. Experiments are currently in progress to determine if lipid demixing also occurs in more complex lipid mixtures (DOPE, DOPC, sterols and cerebrosides at proportions similar to the rye plasma membrane) at those hydrations that occur during freezing over the range of -10°C to -40°C.

Acknowledgements

We wish to thank Dr. Gary Bryant for kindly providing a copy of his Ph.D. thesis. This work was supported by U.S. Department of Energy Grant No. DE-FG02-84ER13214 to P.L.S., National Institutes of Health Grant No. GM28120 to S.W.H., and by a Natural Sciences and Engineering Research Council of Canada Postdoctoral Fellowship to M.S.W.

References

1 Steponkus, P.L. and Lynch, D.V. (1989) J. Bioenerg. Biomembr. 21, 21–41.
2 Steponkus, P.L., Lynch, D.V. and Uemura, M. (1990) Phil. Trans. R. Soc. Lond. B 326, 571–583.
3 Gordon-Kamm, W.J. and Steponkus, P.L. (1984) Proc. Natl. Acad. Sci. USA 81, 6373–6377.
4 Sugawara, Y. and Steponkus, P.L. (1990) Cryobiology 27, 667.
5 Lynch, D.V. and Steponkus, P.L. (1987) Plant Physiol. 83, 761–767.
6 Crowe, J.H. and Crowe, L.M. (1984) in Biological Membranes (Chapman, D., ed.), Vol. 5, pp. 57–103, Academic Press, London.
7 Lynch, D.V. and Steponkus, P.L. (1989) Biochim. Biophys. Acta 984, 267–272.
8 Bryant, G. and Wolfe, J. (1989) Eur. Biophys. J. 16, 369–372.
9 Rand, R.P. (1981) Annu. Rev. Biophys. Bioengen. 10, 277–314.
10 Gruner, S.M. (1989) J. Phys. Chem. 93, 7562–7570.
11 Luzzati, V., Gulik-Krzywicki, T. and Tardieu, A. (1968) Nature (Lond.) 218, 1031–1034.

12 Rockland, L.B. (1960) Anal. Chem. 32, 1375–1376.
13 Rand, R.P. and Parsegian, V.A. (1989) Biochim. Biophys. Acta 988, 351–376.
14 Rand, R.P., Fuller, N.L., Gruner, S.M. and Parsegian, V.A. (1990) Biochemistry 29, 76–87.
15 Lis, L.J., McAlister, M., Fuller, N., Rand, R.P. and Parsegian, V.A. (1982) Biophys. J. 37, 657–666.
16 Gruner, S.M., Tate, M.W., Kirk, G.L., So, P.T.C., Turner, D.C., Keane, D.T., Tilcock, C.P.S. and Cullis, P.R. (1988) Biochemistry 27, 2853–2866.
17 Sen, A. and Hui, S.W. (1988) Chem. Phys. Lipids 49, 179–184.
18 Seddon, J.M. (1990) Biochim. Biophys. Acta 1031, 1–69.
19 Tate, M.W. and Gruner, S.M. (1987) Biochemistry 26, 231–236.
20 Marsh, D. (1990) CRC Handbook of Lipid Bilayers, pp. 135–158, CRC Press, Boca Raton.
21 Chapman, D. (1975) Q. Rev. Biophys. 8, 185–235.
22 Bryant, G.L. (1991) Ph.D. thesis, The University of New South Wales, Sydney, Australia.
23 Tamura-Lis, W., Reber, E.J., Cunningham, B.A., Collins, J.M. and Lis, L.J. (1986) Chem. Phys. Lipids 39, 119–124.
24 Marra, J. and Israelachvili, J. (1985) Biochemistry 24, 4608–4618.
25 Eriksson, P.-O., Rilfors, L., Lindblom, G., and Arvidson, G. (1985) Chem. Phys. Lipids 37, 357–371.
26 Bradshaw, J.P., Edenborough, M.S., Sizer, P.J.H., and Watts, A. (1989) Biochim. Biophys. Acta 987, 104–110.
27 Tate, M.W. and Gruner, S.M. (1989) Biochemistry 28, 4245–4253.
28 Hui, S.W. and Sen, A. (1989) Proc. Natl. Acad. Sci. USA 86, 5825–5829.